

Dielectric suppression of nanosolid silicon

L K Pan, Chang Q Sun¹, T P Chen, S Li, C M Li and B K Tay

School of Electrical and Electronic Engineering, Nanyang Technological University, 639798, Singapore

E-mail: ecqsun@ntu.edu.sg

Received 1 October 2004, in final form 4 October 2004

Published 15 November 2004

Online at stacks.iop.org/Nano/15/1802

doi:10.1088/0957-4484/15/12/019

Abstract

An analytical solution is presented showing that the dielectric susceptibility of a nanosolid depends functionally on the crystal binding that determines the bandgap and hence the essential processes of electron polarization, and on the electron–phonon coupling, that is often overlooked in theory considerations. The derived solution covers all the measured values of bandgap expansion that are beyond the reach of available approaches. Consistency between predictions and impedance measurements evidences the impact of atomic coordination-number imperfection on the dielectric performance of nanometric semiconductors and the validity of the given solution.

1. Introduction

Miniaturizing a semiconductor down to nanometre scale causes the bandgap (E_G) to expand [1–3] and the inner core-level to shift [4, 5] towards higher binding energy. The dielectric constant ϵ_r of the semiconductor is no longer constant but decreases with solid size [6–8]. The reduced ϵ_r has enormous impact on the electrical and optical performance of the solid and the related devices. For instance, the ϵ_r reduction enhances the Coulomb interaction between charged particles such as electrons, holes, and ionized shallow impurities in nanometric devices, leading to abnormal responses of the devices. The increase in the energies for exciton (electron–hole pair) activation in nanometric semiconductors due to ϵ_r reduction would significantly influence optical absorption and transport properties of these devices.

Conventionally, the dielectric response of a porous Si (p-Si) is described by the effective medium approximations [9, 10], that simply average the dielectric contribution from the air pores and the backbones of the silicon (nano-Si). The dielectrics of a nano-Si is often presumed to take the bulk constant and the $\epsilon_{\text{nano-Si}}$ can be derived from the measured ϵ_{eff} of a p-Si by using the simple Looygenga formula [11]:

$$\epsilon_{\text{eff}}^{1/3} = (1 - p)\epsilon_{\text{nano-Si}}^{1/3} + p\epsilon_{\text{air}}^{1/3}, \quad (1)$$

where ϵ_{air} (≈ 1) is the dielectric constant of air and p the porosity of the p-Si. However, this approach ignores the

fact that the dielectric constant of a nano-Si is not only lower than the bulk value but also size dependent [8]. Contribution from the lower-coordinated surface atoms cannot be neglected in accounting for the dielectric performance of the p-Si, in particular at very small sizes [12]. Therefore, the effective medium methods need to be modified by taking account of the size-dependent dielectric performance of the nano-Si backbones, $\epsilon_{\text{nano-Si}}$.

There have been several models to describe the size-dependence of the real part of the dielectric constant, $\epsilon_r(K)$ of a nanosolid with diameter D (we prefer the dimensionless form of $K = D/2d$ that is the number of atoms lined along the radius of the nanodot; $d = 0.2632$ nm is the diameter of a bulk Si atom) with a lack of models for the complex dielectric constant. The relative change of the dielectric susceptibility, $\chi = \epsilon_r - 1$, can be modelled as

$$\frac{\Delta\chi(K)}{\chi(\infty)} = \begin{cases} -[1 + (K/\alpha)^\lambda]^{-1} & \text{(Penn)} \\ -2\Delta E_G(K)/E_G(\infty) & \text{(Tsu)} \\ -\frac{2}{1 - (E/E_G(\infty))^2} \left(\frac{\Delta E_G(K)}{E_G(\infty)} \right) & \text{(Chen)} \end{cases} \quad (2)$$

where α and λ are freely adjustable parameters used for fitting the measured data in the Penn empirical model [13]. Tsu *et al* [14] relate the susceptibility change directly to the $E_G(K)$. Considering the photon energy, Chen *et al* [15]

¹ <http://www.ntu.edu.sg/home/ecqsun/>

modified the Tsu model and studied the dielectric properties of nanosolid Si embedded in SiO₂ matrix. Both the Tsu and Chen approximations relate the dielectric suppression directly to the E_G expansion. However, recent calculations by Delerue *et al* [16] suggested that the decrease of the average dielectric response with decreasing size is due to the breaking of polarizable bonds at the surface instead of the E_G expansion. Actually, contributions from surface atoms and contributions from core atoms to the dielectrics are very different. As noted by Chen, the models of Tsu and Chen [14, 15] are valid only at $\Delta E_G(K)/E_G(\infty) \ll 0.5$; otherwise, $\chi(K)$ becomes negative. It happens quite often that E_G expands beyond this critical value. For instance, the E_G of Si nanorods increases from 1.1 to 3.5 eV with decreasing the rod diameter from 7.0 to 1.3 nm and the surface Si–Si bond contracts by $\sim 12\%$ from the bulk value (0.263 nm) to ~ 0.23 nm [1]. Furthermore, electron–phonon interaction becomes increasingly important when the solid size is in the nanometre range [17, 18]. The electron–phonon coupling contributes to the process of electron polarization [19], which has been overlooked in previous considerations. Therefore, deeper insight into the origin and a clearer numerical expression involving the contribution from electron–phonon coupling for the dielectric performance of a nanosolid semiconductor is highly desirable. Here we present an analytical expression for the suppression of complex dielectrics as a whole by solving the Kramers–Kronig relation that involves electron–phonon interaction. The derived relation is further verified by comparing the measurement of dielectrics of porous Si. Agreement between predictions and the experimental data documented in the literature and the current measurement shows that the dielectric susceptibility of a nanosolid depends on the extent of both the crystal binding and the electron–phonon coupling, both of which change with solid size. The size dependences of the crystal binding and the electron–phonon coupling are dictated by the atomic coordination-number (CN) imperfection, the effect of which follows the recent bond-order–length–strength (BOLS) correlation mechanism [2–5].

2. Model

The BOLS correlation developed from the bond-order–length notations of Goldschmidt [20] and Pauling [21], as detailed in [4], indicates that the CN imperfection of an atom in the surface region results in the remaining bonds of the lower-coordinated atom contracting spontaneously with an associated magnitude increase of the binding energy [2–5]. For interfacial atoms, the CN changes a little but the bond nature alternates. Bond nature alteration (compound or alloy formation) also strengthens the interfacial bonds. The bond strength enhancement contributes not only to the atomic cohesive energy (E_{coh} , single-bond energy multiplies the atomic CN) of the specific atom but also to the energy density in the relaxed surface region. The atomic cohesive energy contributes to the Gibbs free energy that determines the thermodynamic behaviour of the system such as critical temperatures for phase transition [22], liquidation and evaporation [23] of a nanosolid as well as the activation energies for atomic diffusion, atomic dislocation [24] and chemical reaction. The binding energy density increase

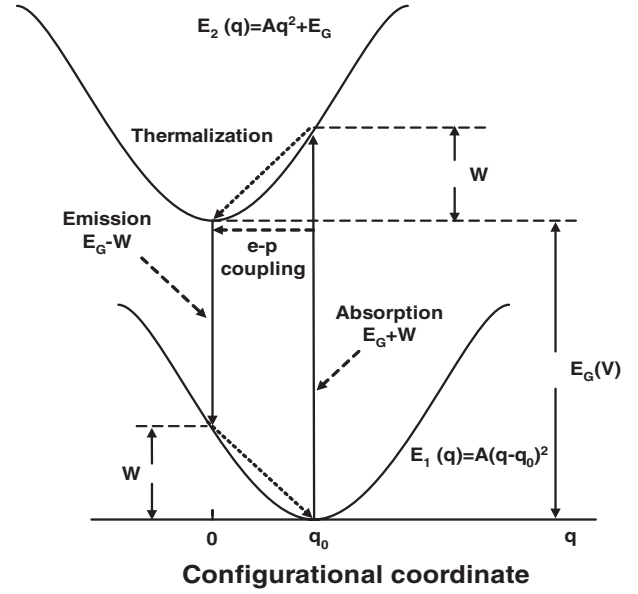


Figure 1. Mechanism for photo-absorption and photo-emission of a nanometric semiconductor involving crystal binding (E_G) and electron–phonon coupling (W) [19]. The electron is excited by absorbing a photon with energy $E_G + W$ from the ground minimum to the excited state and then undergoes a thermalization to the excited minimum and finally transmits again to the ground by emitting a photon with energy $E_G - W$.

perturbs the Hamiltonian of an extended solid that determines the entire band structure such as the bandgap, core-level shift and bandwidth. The joint effect of cohesive energy and binding energy density determines the mechanical strength of the system as well [25]. According to the BOLS correlation, the blue shift in photoluminescence and the dielectric suppression of a nanosolid are consequences of the atomic CN imperfection. Surface chemical passivation also affects the band structure and dielectric performance [26], but in the current study we focus on the physical size effect.

The static dielectric constant originates from electronic polarization, or electron transition from the lower valence band to the upper conduction band. This process is subject to the selection rule of energy and momentum conservation, which determines the optical response of semiconductors and reflects how strongly the valence electrons couple with the excited conduction electrons [27]. Therefore, the ϵ_r of a semiconductor is directly related to its E_G at room temperature (RT). Determination and discussion of the effect of electron–phonon coupling on the band structure [19] (as illustrated in figure 1) has formed the subject of [17].

The energy difference between the conduction band $E_C(q)$ and valence band $E_V(q)$ at q is given as

$$\begin{aligned} E_C(q) - E_V(q) &= \hbar\omega = E_2(q) - E_1(q) \\ &= E_G - Aq_0^2 + 2Aqq_0 \\ &= E_{\text{PL}} + 2Aqq_0 \end{aligned} \quad (3)$$

where \hbar is the Planck constant, ω is the frequency and E_{PL} is the photoluminescence (PL) peak energy. The energies of the ground state $E_1(q) = A(q - q_0)^2$ and the excited state $E_2(q) = Aq^2 + E_G$ are functions of a configurational coordinate, q , which is in the wavevector dimension. Constant A determines the shape of the energy curve. q_0 is inversely proportional

to the atomic distance d_i : $q_0 \propto d_i^{-1}$. The imaginary part of the complex dielectric constant $\varepsilon'_r(\omega)$ describes the electromagnetic wave absorption and is responsible for the energy loss of incident irradiation by electron excitation. The imaginary part of the complex dielectric constant can be obtained by inserting equation (3) into the relation [28, 29]

$$\begin{aligned}\varepsilon'_r(\omega) &= \frac{F}{\omega^2} \int ds \frac{f_{CV}}{|\nabla_q[E_C(q) - E_V(q)]|} \\ &= \frac{\pi F f_{CV}}{A\omega^2} q \\ &= \frac{\pi F f_{CV} \hbar\omega - E_{PL}}{2A^2 q_0\omega^2}, \quad (ds = 2\pi q_0 dq) \quad (4)\end{aligned}$$

where s is the area difference between the two curved surfaces in q space of the upper and the lower bands. F is a constant and ∇_q the gradient in q space. f_{CV} , the probability of inter-subband transition, varies insignificantly with particle size in the first order approximation, in particular for particles containing hundreds atoms or over. The size-induced change of inter-subband transition probability is negligibly small because it originates from the Kubo sublevel expansion in the valence and the conduction band. For particles containing hundreds of atoms or more, the Kubo expansion is negligibly small.

The Kramers–Kronig relation correlates the real part to the imaginary part of the dielectric constant $\varepsilon'_r(\omega)$ [30],

$$\begin{aligned}\varepsilon_r(0) - 1 = \chi &= \frac{2}{\pi} \int_{\omega_0}^{\infty} \frac{\varepsilon'_r(\omega)}{\omega} d\omega \quad (\omega_0 = E_{PL}/\hbar) \\ &= \frac{F f_{CV}}{A^2 q_0} \int_{\omega_0}^{\infty} \frac{\hbar\omega - E_{PL}}{\omega^3} d\omega \\ &= \frac{G}{q_0 E_{PL}}, \quad (G = \hbar^2 F f_{CV}/2A^2). \quad (5)\end{aligned}$$

Hence, the size-depressed dielectric susceptibility depends functionally on the characteristics of electron–phonon interaction (q_0) and the photoluminescence energy, which is in contrast with the relations given in equation (2). The relative change of the susceptibility and the imaginary part of the dielectrics are derived as follows [4]:

$$\begin{aligned}\frac{\Delta\chi(K)}{\chi(\infty)} &= -\frac{\Delta E_{PL}(K)}{E_{PL}(\infty)} - \frac{\Delta q_0}{q} \\ &= -\frac{\Delta E_{PL}(K)}{E_{PL}(\infty)} + \frac{\Delta d_i}{d} \\ &= -(\Delta_H - B\Delta_{e-p}) + \Delta_d, \quad (6) \\ \frac{\Delta\varepsilon'_r(K, \omega)}{\varepsilon'_r(\infty)} &= \frac{-E_{PL}(\infty)}{\hbar\omega - E_{PL}(\infty)} \frac{\Delta E_{PL}(K)}{E_{PL}(\infty)} + \frac{\Delta d_i(K)}{d_0} \\ &= \frac{-E_{PL}(\infty)}{\hbar\omega - E_{PL}(\infty)} (\Delta_H - B\Delta_{e-p}) + \Delta_d\end{aligned}$$

where B is the electron–phonon coupling coefficient. Δ_H , Δ_{e-p} and Δ_d represent the contribution from the CN imperfection perturbed Hamiltonian, the electron–phonon coupling and the bond length in the relaxed region. Δ_H , Δ_{e-p}

and Δ_d are given as [2, 4]:

$$\begin{aligned}\Delta_H &= \sum_3 \gamma_i (c_i^{-m} - 1); & \Delta_{e-p} &= \sum_3 \gamma_i (c_i^{-2} - 1); \\ \Delta_d &= \sum_3 \gamma_i (c_i - 1); & z_1 &= 4(1 - 0.75/K)\end{aligned}$$

$$c_i = 2/\{1 + \exp[(12 - z_i)/(8z_i)]\} \quad \gamma_i = V_i/V = N_i/N \quad (7)$$

where c_i is the bond contraction coefficient that formulated Goldschmidt's notation. γ_i is the surface-to-volume ratio and z_1 is the curvature dependence of the atomic CN in the outermost atomic layer. For a silicon spherical dot [4], $B = 0.91$, $m = 4.88$, $z_2 = 6$, and $z_3 = 12$. Subscript i denotes the specific i th atom of concern, which is counted from the outermost atomic layer to the centre of the solid. It is possible now to discriminate the dielectric contribution of the nanosolid Si backbone from the measured effective ε_{eff} of p-Si by matching the prediction with the measured impedance.

The absorption coefficient, α , the refractive index, $n (= \sqrt{\varepsilon_r})$, and the complex dielectric function are correlated as $\alpha(\omega) = 2\pi\varepsilon'_r(\omega)/n\lambda$ (λ is wavelength), and the transmittance of light is given as $T \propto \exp(-\alpha x)$, where x is the thickness of the medium for light transmission. This leads to the size-induced change of α as

$$\begin{aligned}\frac{\Delta\alpha(K, \omega)}{\alpha(\infty, \omega)} &= \frac{\Delta\varepsilon'_r(K, \omega)}{\varepsilon'_r(\infty, \omega)} - \frac{\Delta\varepsilon_r(K)}{2\varepsilon_r(\infty)} \\ &= -\left[\frac{\chi(\infty)}{\chi(\infty) + 1} + \frac{\alpha' E_G(\infty)}{\hbar\omega - E_G(\infty)} \right] \Delta_H \quad (\text{convention}) \\ \text{or} &= \left[\frac{\chi(\infty)}{2[\chi(\infty) + 1]} - \frac{E_{PL}(\infty)}{\hbar\omega - E_{PL}(\infty)} \right] \\ &\times (\Delta_H - B\Delta_{e-p}) + \frac{\chi(\infty) + 2}{2[\chi(\infty) + 1]} \Delta_d \quad (\text{BOLS}). \quad (8)\end{aligned}$$

The traditional form $[\Delta\chi(K)/\chi(\infty) = -2\Delta_H]$ discriminates the direct and indirect bandgap transition by the α' while the BOLS form (equation (6)) counts the e–p coupling, lattice contracting and crystal binding.

3. Experiment

We prepared the p-Si samples² and measured their impedance in the frequency range of 50 Hz–1.0 MHz under an applied potential of 100 mV, using a Fluke PM–6303 resistance–capacitance–inductance (*RCL*) meter with a four-wire probe. All the measurements were carried out in atmospheric ambient. Silver paste was used as an ohmic contact to both p-Si and Si substrate. The resistance contribution from Si substrate could be neglected [31, 32] due to the high conductivity of bulk Si compared to the p-Si.

² The PS samples were prepared on a p-type (100) Si wafer with resistivity of 1–25 Ω cm at room temperature. Electrolyses were performed by an galvanostat in HF:C₂H₅OH:H₂O solution, where the weight ratios were 1:5:4. Samples A, B, C, D and E were obtained by applying the current densities of 80, 60, 50, 40 and 30 mA cm⁻² for 10 min, respectively. The porosities and particle sizes of PS were determined through weight measurement and by matching the measured peak energy E_{PL} in photoluminescence (PL) with the predicted size-dependent PL profile that matches numerous sets of PL data on PS, CdS and CdSe nanosolids reported by others.

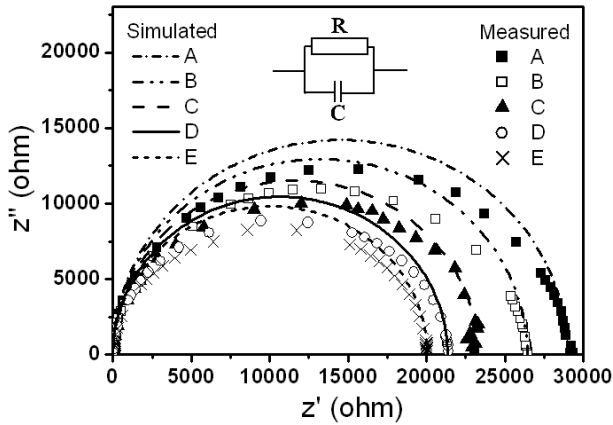


Figure 2. Size dependent Cole–Cole plots of p-Si. The dots represent the data measured by the *RCL* meter at RT and the lines correspond to simulation using the *RC* parallel circuit model (inset) for typical dielectric materials.

4. Results and discussion

The impedance behaviour can be described by Debye's expression of a parallel *RC* circuit [33] with elements that correspond to the dielectric behaviour of the bulk grain, as shown in the inset of figure 2. The complex impedance Z^* measured by the *RCL* meter can be expressed as

$$\begin{aligned} Z^* &= Z' - jZ'', \\ Z' &= \frac{R}{1 + \omega^2 R^2 C^2}, \\ Z'' &= \frac{\omega R^2 C}{1 + \omega^2 R^2 C^2}, \end{aligned} \quad (9)$$

where ω is the angular frequency. Here the bulk-grain resistance R represents ionic or electronic conduction mechanisms, while the capacitance C represents the polarizability of the p-Si. The complex impedance response commonly exhibits a semicircular form in the measured Cole–Cole plot [34] as shown in figure 2. A–E denote the responses of different samples (table 1) measured at RT. The complex impedance plots show only one depressed single semicircular arc, indicating that only one primary mechanism, corresponding to the bulk grain behaviour, dominates at RT for polarization within the p-Si film. At higher temperature, two or more semicircles present corresponding different transition mechanisms [12, 32]. The second intercept on the real axis made by the semicircle corresponds to the resistance in the bulk grain. As can be seen, the intercept of the semicircles shifts towards the origin as the nanosolid size increases, indicating a reduction of the bulk grain resistance.

The way [35] to extract the capacitance and dielectric constant is by using the equation: $Z'' = 1/(\omega C)$ in the high frequency range (10^5 – 10^6 Hz). The bulk grain capacitance C of the sample is given by the slope of the straight line determined by the variation of Z'' as a function of $1/\omega$. Then, the effective dielectric constant ϵ_{eff} of the porous structure is calculated based on the equation $\epsilon_{\text{eff}} = Cl/(\epsilon_0 S)$. ϵ_0 is the dielectric constant of a vacuum, l is the thickness of the sample (10–15 μm) that was measured from the cross

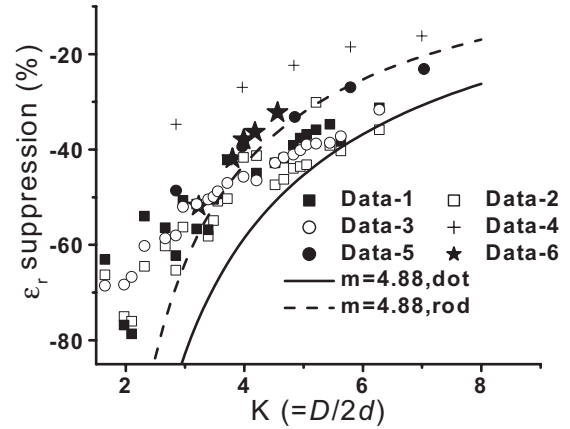


Figure 3. Comparison of the predictions on the size-dependent dielectric constants of silicon nanosolids with the sophisticated calculation and measurement results. Calculated data 1, 2, 3 are after [36]. Calculated data 4 and 5 are after [6]. Data 6 is the current experimental results. d is the bond length of bulk silicon. K is the number of atoms arranged along the radius of a spherical dot or a rod.

Table 1. Summary of the D -dependent $\epsilon_{\text{nano-Si}}$ derived from the measured E_{PL} , porosity and ϵ_{eff} , p-Si. The porosities and D of PS were determined through weight measurement and by matching the measured peak energy E_{PL} in PL with the predicted size-dependent PL profile that matches numerous sets of PL data on PS, CdS and CdSe nanosolids reported by others [2, 3].

Sample	D (nm)	E_{PL} (eV)	Porosity (%)	ϵ_{eff}	$\epsilon_{\text{nano-Si}}$
A	1.7	2.08	85	1.43	6.27
B	2.0	1.82	76	1.84	7.29
C	2.1	1.81	71	2.11	7.7
D	2.2	1.79	68	2.28	7.86
E	2.4	1.76	66	2.45	8.29

section of the sample by scanning electron microscope; S is the area of the silver electrode (250 mm²). With the measured ϵ_{eff} , we can calculate the $\epsilon_{\text{nano-Si}}$ based on the Looyenga formula (equation (1)). The measured ϵ_{eff} and derived $\epsilon_{\text{nano-Si}}$ for different sizes are listed in table 1. It is not surprising that $\epsilon_{\text{nano-Si}}$ is much higher than the ϵ_{eff} due to the void ($\epsilon_{\text{air}} \approx 1$) involvement. $\epsilon_{\text{nano-Si}}$ decreases with solid size due to the atomic CN imperfection and hence it is not appropriate to simply take the bulk value as $\epsilon_{\text{nano-Si}}$ in conventional calculations. Figure 3 compares the $\epsilon_{\text{nano-Si}}$ derived herewith using the aforementioned approach with the BOLS predicted size-dependence and other sophisticated calculations of nanosolid Si.

Other factors may contribute to dielectric suppression, which makes the prediction deviate from measurement compared with other simulations reported by this group. One apparent factor is the accuracy and uniformity of the shape and size of porous Si. For example, atomic CN at a negatively curved surface of a pore is higher than that at the positively curved surface of a dot. The numerical solution sums the contribution from crystal binding (E_G expansion), electron–phonon coupling and bond contraction, which may accumulate the three categories, contributing to the observed deviation. However, from a physical and chemical insight point of view, the first (main) order approximation would be acceptable as

other artifacts from measurement or impurities are hardly controllable.

5. Conclusions

In summary, incorporating the BOLS correlation into the mechanism for electron polarization and the dielectric Kramers–Kronig relation has enabled the dielectric suppression of silicon nanosolids to be formulated and understood in terms of the often-overlooked event of surface CN imperfection and its effect on the crystal binding and the electron–phonon coupling due to atomic CN imperfection. The analytical form covers all the possible values of E_G expansion. Consistency between BOLS predictions and the measured results evidences that the BOLS correlation describes adequately the true situation in which the $\epsilon_{\text{nano-Si}}$ suppression is dictated by atomic CN imperfection that provides impact on the interatomic interaction and electron–phonon coupling. Matching predictions to the experimental observations verifies the validity and essentiality of the approach as well as the Looyenga relation.

References

- [1] Ma D D D, Lee C S, Au F C K, Tong S Y and Lee S T 2003 *Science* **299** 1874
- [2] Pan L K, Sun C Q, Tay B K, Chen T P and Li S 2002 *J. Phys. Chem. B* **106** 11725
- [3] Sun C Q, Li S, Tay B K and Chen T P 2002 *Acta Mater.* **50** 4687
- [4] Sun C Q 2004 *Phys. Rev. B* **69** 045105
- [5] Sun C Q, Pan L K, Fu Y Q, Tay B K and Li S 2003 *J. Phys. Chem. B* **107** 5113
- [6] Wang L L and Zunger A 1994 *Phys. Rev. Lett.* **73** 1039
- [7] Walter J P and Cohen M L 1970 *Phys. Rev. B* **2** 1821
- [8] Sun C Q, Sun X W, Tay B K, Lau S P, Huang H and Li S 2001 *J. Phys. D: Appl. Phys.* **34** 2359
- [9] Pickering C, Beale M J, Robbins D J, Pearson P J and Greef R 1984 *J. Phys. C: Solid State Phys.* **17** 6535
- [10] Ferrieu F, Hallimaoui A and Bensahel D 1992 *Solid State Commun.* **84** 293
- [11] Looyenga H 1965 *Physica* **31** 401
- [12] Pan L K, Huang H T and Sun C Q 2003 *J. Appl. Phys.* **94** 2695
- [13] Penn D R 1962 *Phys. Rev. B* **128** 2093
- [14] Tsu R and Babic D 1994 *Appl. Phys. Lett.* **64** 1806
- [15] Chen T P, Liu Y, Tse M S, Tan O K, Ho P F, Liu K Y, Gui D and Tan A L K 2003 *Phys. Rev. B* **68** 153301
- [16] Delerue C, Lannoo M and Allan G 2003 *Phys. Rev. B* **68** 115411
- [17] Pan L K and Sun C Q 2004 *J. Appl. Phys.* **95** 3819
- [18] Micici O I and Nozik A J 2002 *The Nanostructures Materials and Technology* ed H S Nalwa (New York: Academic) chapter 5, p 183
- [19] Street R A 1991 *Hydrogenated Amorphous Silicon* (Cambridge: Cambridge University Press) p 279
- [20] Goldschmidt V M 1927 *Ber. Deut. Chem. Ges.* **60** 1270
- [21] Pauling L 1947 *J. Am. Chem. Soc.* **69** 542
- [22] Feibelman P J 1996 *Phys. Rev. B* **53** 13740
- [23] Zhong W H, Sun C Q, Tay B K, Li S, Bai H L and Jiang E Y 2002 *J. Phys.: Condens. Matter* **14** L399
- [24] Sun C Q, Wang Y, Tay B K, Li S, Huang H and Zhang Y 2002 *J. Phys. Chem. B* **106** 10701
- [25] Sun C Q, Li C M, Li S and Tay B K 2004 *Phys. Rev. B* **69** 245402
- [26] Sun C Q, Tay B K, Lau S P, Sun X W, Zeng X T, Bai H, Liu H, Liu Z H and Jiang E Y 2001 *J. Appl. Phys.* **90** 2615
- [27] Sun C Q 2003 *Prog. Mater. Sci.* **48** 521
- [28] Canham L 1997 *Properties of Porous Silicon* (London: INSPEC) p 234
- [29] Omar M A 1975 *Elementary Solid State Physics: Principles and Applications* (New York: Addison-Wesley) p 403
- [30] Greenway D L and Harbecke G 1968 *Optical Properties and Band Structure of Semiconductors* (New York: Pergamon)
- [31] Brown F G 1968 *The Physics of Solids* (New York: Benjamin)
- [32] Miyata K and Dreifus D L 1994 *Japan. J. Appl. Phys.* **1** **33** 4526
- [33] Ye H T, Sun C Q, Huang H T and Hing P 2001 *Appl. Phys. Lett.* **78** 1826
- [34] Macdonald J R 1987 *Impedance Spectroscopy* (New York: Wiley) chapter 4
- [35] Orton J W and Powell M J 1980 *Rep. Prog. Phys.* **43** 1266
- [36] Lanfredi S, Carvalho J F and Hernandez A C 2000 *J. Appl. Phys.* **88** 283
- [37] Lannoo M, Delerue C and Allan G 1995 *Phys. Rev. Lett.* **74** 3415